

A novel method for nonstationary power spectral density estimation of cardiovascular pressure signals based on a Kalman filter with variable number of measurements

Z. G. Zhang · K. M. Tsui · S. C. Chan ·
W. Y. Lau · M. Abov

Received: 25 July 2007 / Accepted: 17 April 2008 / Published online: 22 May 2008
© International Federation for Medical and Biological Engineering 2008

Abstract We present a novel parametric power spectral density (PSD) estimation algorithm for nonstationary signals based on a Kalman filter with variable number of measurements (KFVNM). The nonstationary signals under consideration are modeled as time-varying autoregressive (AR) processes. The proposed algorithm uses a block of measurements to estimate the time-varying AR coefficients and obtains high-resolution PSD estimates. The intersection of confidence intervals (ICI) rule is incorporated into the algorithm to generate a PSD with adaptive window size from a series of PSDs with different number of measurements. We report the results of a quantitative assessment study and show an illustrative example involving the application of the algorithm to intracranial pressure signals (ICP) from patients with traumatic brain injury (TBI).

Keywords Cardiovascular pressure signal · Kalman filter · Power spectral density · Time-varying autoregressive process · Traumatic brain injury

1 Introduction

Power spectral density (PSD) estimation is widely used in the analysis of biomedical signals [3, 15]. There are two general frameworks of PSD estimation: nonparametric and parametric methods [7, 12, 13]. Nonparametric PSD estimation methods do not assume a particular model for the signal under analysis and estimate the spectrum directly from the data. These methods are capable of providing unbiased estimation of the PSD if a sufficiently large number of independent observations are available. On the other hand, parametric methods assume the signals under analysis can be modeled as the output of a linear system where the input is white noise. In general, nonparametric methods have lower computational complexity than parametric methods, while parametric methods can provide higher frequency resolutions if the observations can be adequately explained by the model and the SNR is sufficiently high [10].

The above-mentioned methods assume that the signal under analysis is stationary and its statistics such as mean, variance, and autocorrelation do not change with time. However, most biomedical signals, such as the cardiovascular pressure signals considered in this work, contain numerous nonstationary or transient characteristics such as drifts, trends, abrupt changes, and beginnings and ends of clinical events. To understand the time-frequency properties of such nonstationary signals, several time-varying PSD estimation methods have been developed based on nonparametric spectrum estimation such as the spectrogram, scalogram [11, 14], Wigner distribution and its variants [4, 16]. Similarly, parametric spectrum estimations algorithms have been proposed using a Kalman filter framework [8, 9]. It has been shown that parametric PSD estimation methods may result in higher time-frequency

Z. G. Zhang (✉)
Department of Orthopaedics and Traumatology,
and Department of Electrical and Electronic Engineering,
The University of Hong Kong, Pokfulam Road,
Hong Kong, China
e-mail: zgzhang@eee.hku.hk

K. M. Tsui · S. C. Chan · W. Y. Lau
Department of Electrical and Electronic Engineering,
The University of Hong Kong, Pokfulam Road,
Hong Kong, China

M. Abov
Department of Electronics Engineering Technology,
Oregon Institute of Technology, Portland, OR, USA

resolutions than nonparametric PSD estimations when the SNR is high enough [8, 9]. In these methods, the nonstationary signals are treated as a smoothness prior AR process where the time-varying AR coefficients are described by a stochastically perturbed difference equation constraint model. A Kalman filter is then used to track the AR coefficients and estimate the time-varying PSD estimation.

Recently, a Kalman filter-based PSD estimation algorithm similar to the work in [8, 9] was developed for nonstationary signals and applied to cardiovascular pressure signals such as arterial blood pressure (ABP) and intracranial pressure (ICP) signals [1, 2]. The main limitation of this method is the fact that it only employs the current measurement to update the AR coefficients, which results in AR coefficient estimates with large variance. To solve this problem, a simple averaging operation over short time windows was employed in [1]. However, the averaging operation blurs the time resolution to a certain extent. This is a fundamental problem in PSD estimation that is referred to as the time-frequency resolution tradeoff [7]. A measurement window of appropriate length can help to reduce the estimation variance, while avoiding excessive bias for nonstationary signals. A long window is preferred for slow-varying frequency contents to reduce the estimation variance. Hence, a high frequency resolution (i.e. the ability to correctly resolve adjacent sinusoids) is obtained at the expense of time resolution (i.e. the ability to correctly resolve adjacent events in time). On the contrary, for fast changing frequency components, smaller windows are desirable in order to reduce the bias error. As a result, better time resolution is achieved for tracking the fast varying frequency content, but the frequency resolution will be degraded.

In this paper we propose a new parametric PSD estimation algorithm based on a Kalman filter that uses a variable number of measurements (KFVNM). The nonstationary time series are first modeled by a time-varying AR model with prior constraints on the AR coefficients to model the dynamics of the AR coefficients. The smoothness priors are imposed to the AR coefficients using a stochastically perturbed model, which can be expressed in the form of an independent white noise excited difference equation with constraints on each AR coefficient. These difference equations are then incorporated as a state-space representation so that the AR coefficients can be determined using the Kalman filter framework. Unlike the conventional Kalman filter, the proposed KFVNM algorithm employs a block of measurements to achieve a better tradeoff between the bias and variance of the estimated AR coefficients, and hence a higher accuracy of the time-frequency contents. To address the window selection problem, our proposed method uses the intersection of confidence intervals (ICI)

rule, which has been successfully applied to the Wigner distribution [16]. This enables the proposed KFVNM algorithm to determine the window size adaptively. The problem of PSD estimation involving nonstationary pressure signals is used in an illustrative example to illustrate the effectiveness of the proposed approach. Our simulation results show that the proposed PSD estimation algorithm provides better time-frequency resolution than conventional Kalman filter-based algorithms for the time-varying synthetic pressure signal tested. Similar observations are found for real pressure signals.

2 Methods

2.1 Kalman filter-based PSD estimation

The Kalman filter framework of PSD estimation typically assumes the signals under analysis are nonstationary and can be characterized by a time-varying AR process as follows:

$$y(t) = \sum_{i=1}^M a(i, t)y(t-i) + \varepsilon(t), \quad (1)$$

where M is the order of the AR model, $a(i, t)$ are the time-varying AR coefficients and $\varepsilon(t)$ is assumed to be a zero mean Gaussian white noise sequence with variance σ_ε^2 . To describe the variation of the AR coefficients, a stochastically perturbed κ -th order difference equation constraint model is employed [8, 9]:

$$\nabla^\kappa a(i, t) = \delta(i, t), \quad i = 1, \dots, M, \quad (2)$$

where $\delta(i, t)$ is assumed to be a zero mean Gaussian white noise sequence with variance $\sigma_{\delta, i}^2 = \sigma_\delta^2$, $i = 1, \dots, M$. For simplicity, κ is assumed to be one in this paper. The difference equation constraint in Eq. 2 becomes a first-order AR process with $\delta(i, t)$ as the innovation vector:

$$a(i, t) = a(i, t-1) + \delta(i, t). \quad (3)$$

The AR model for the nonstationary signal in Eq. 1 and the first-order difference equation constraint model in Eq. 3 can be incorporated into the following discrete-time linear state-space model as:

$$\mathbf{x}(t) = \mathbf{F}(t)\mathbf{x}(t-1) + \boldsymbol{\delta}(t), \quad (4)$$

$$y(t) = \mathbf{H}(t)\mathbf{x}(t) + \varepsilon(t). \quad (5)$$

In the above state-space model, the state vector $\mathbf{x}(t)$ is defined as $\mathbf{x}(t) = [a(1, t), \dots, a(M, t)]^T$, and $y(t)$ is the observation or measurement. The observation matrix and state transition matrix are respectively given as $\mathbf{H}(t) = [y(t-1), \dots, y(t-M)]$ and $\mathbf{F}(t) = \mathbf{I}_M$, where \mathbf{I}_M is an $M \times M$ identity matrix. The state noise vector is $\boldsymbol{\delta}(t) = [\delta(1, t), \dots, \delta(M, t)]^T$ with covariance matrix $\mathbf{Q}(t) = \sigma_\delta^2 \mathbf{I}_M$,

and $\varepsilon(t)$ is the measurement noise with covariance $\mathbf{R}(t) = \sigma_\varepsilon^2$.

Given the linear state-space model composed of Eqs. 4 and 5, the state vector $\mathbf{x}(t)$ or the AR coefficients $a(i, t)$ can be estimated using the Kalman filter recursion. Let $\hat{\mathbf{x}}(t/\tau)$ ($\tau = t-1$ or t) be the estimator of $\mathbf{x}(t)$ given the measurements up to time instant τ , and $\mathbf{P}(t/\tau)$ be the corresponding error covariance matrix of $\hat{\mathbf{x}}(t/\tau)$. The standard Kalman filter recursions are given by:

$$\hat{\mathbf{x}}(t/t-1) = \mathbf{F}(t)\hat{\mathbf{x}}(t-1/t-1), \tag{6}$$

$$\mathbf{P}(t/t-1) = \mathbf{F}(t)\mathbf{P}(t-1/t-1)\mathbf{F}^T(t) + \mathbf{Q}(t), \tag{7}$$

$$e(t) = y(t) - \mathbf{H}(t)\hat{\mathbf{x}}(t/t-1), \tag{8}$$

$$\mathbf{K}(t) = \mathbf{P}(t/t-1)\mathbf{H}^T(t) \cdot [\mathbf{H}(t)\mathbf{P}(t/t-1)\mathbf{H}^T(t) + \mathbf{R}(t)]^{-1}, \tag{9}$$

$$\hat{\mathbf{x}}(t/t) = \hat{\mathbf{x}}(t/t-1) + \mathbf{K}(t)e(t), \tag{10}$$

$$\mathbf{P}(t/t) = [\mathbf{I}_M - \mathbf{K}(t)\mathbf{H}(t)]\mathbf{P}(t/t-1). \tag{11}$$

Finally, using the state estimate $\mathbf{x}(t)$ or $a(i, t)$, a time-frequency representation is given by the changing PSD:

$$Y_{\mathcal{P}}(t, f) = |\mathcal{P}(t, f)|^2, \text{ and } \mathcal{P}(t, f) = \frac{\hat{\sigma}_\varepsilon(t)}{1 - \sum_{i=1}^M a(i, t)e^{-j2\pi fi}} = \frac{\hat{\sigma}_\varepsilon(t)}{1 - e^{H(f)\mathbf{a}(t)}}, \tag{12}$$

where $\mathbf{e}(f) = [e^{-j2\pi f}, \dots, e^{-j2\pi fM}]^T$, $\mathbf{a}(t) = \mathbf{x}(t) = [a(1, t), \dots, a(M, t)]^T$, and $\hat{\sigma}_\varepsilon^2(t)$ is the observation noise variance estimate.

For practical implementation, the observation and state variance matrices can be estimated recursively during the state estimation. First of all, we consider the variance $\mathbf{R}(t) = \sigma_\varepsilon^2(t)$ of the observation noise $\varepsilon(t)$, which can be estimated from $\hat{\varepsilon}(t) = y(t) - \mathbf{H}(t)\hat{\mathbf{x}}(t-1)$. Hence, the variance of $\varepsilon(t)$ can be estimated recursively as:

$$\hat{\sigma}_\varepsilon^2(t) = \lambda_\varepsilon \hat{\sigma}_\varepsilon^2(t-1) + (1 - \lambda_\varepsilon) \hat{\varepsilon}^2(t) \tag{13}$$

where a forgetting factor λ_ε is introduced in the recursive update.

The state noise covariance matrix $\mathbf{Q}(t) = E[\delta(t)\delta^H(t)] = \sigma_\delta^2 \mathbf{I}$ can be estimated using a similar approach. The state noise can be first estimated as $\hat{\delta}(t) = \hat{\mathbf{x}}(t) - \mathbf{F}\hat{\mathbf{x}}(t-1)$, then the state noise variance $\hat{\sigma}_\delta^2$ can be calculated recursively from:

$$\hat{\sigma}_\delta^2(t) = \lambda_\delta \hat{\sigma}_\delta^2(t-1) + (1 - \lambda_\delta) \text{var}[\hat{\delta}(t)] \tag{14}$$

where λ_δ is the forgetting factor and $\text{var}[\hat{\delta}(t)]$ is the variance of state noise vector $\hat{\delta}(t)$ at time instant t . Note the forgetting factors λ_ε and λ_δ should be slightly less than one so that the effects of previous estimations can be gradually neglected. The selection of optimal forgetting factor is

beyond our scope, and thus we set all these forgetting factors to 0.95 in the simulations.

2.2 Kalman filter with variable number of measurements-based PSD estimation

We next describe a new Kalman filter-based PSD estimation algorithm with variable number of measurements (KFVNM). This generalization is intended to achieve a better bias-variance tradeoff in the state tracking and hence representing a clearer time-frequency content of the signal to be analyzed. The proposed KFVNM algorithm is motivated from the work in [5, 10], where a new Kalman filter recursion using the equivalence between the Kalman filter and a particular least-squares (LS) regression problem was proposed. First, we rewrite the linear state-space model in Eqs. 4 and 5 as follows:

$$\begin{bmatrix} \mathbf{I}_M \\ \mathbf{H}(t) \end{bmatrix} \mathbf{x}(t) = \begin{bmatrix} \mathbf{F}(t)\hat{\mathbf{x}}(t-1) \\ y(t) \end{bmatrix} + \mathbf{E}(t), \tag{15}$$

where

$$\mathbf{E}(t) = \begin{bmatrix} \mathbf{F}(t)[\mathbf{x}(t-1) - \hat{\mathbf{x}}(t-1)] + \delta(t) \\ -\varepsilon(t) \end{bmatrix}$$

and

$$E[\mathbf{E}(t)\mathbf{E}^T(t)] = \begin{bmatrix} \mathbf{P}(t/t-1) & 0 \\ 0 & \mathbf{R}(t) \end{bmatrix} = \mathbf{S}(t)\mathbf{S}^T(t).$$

Note that $\mathbf{P}(t/t-1)$ is computed using Eq. 7 and $\mathbf{S}(t)$ is computed from the Cholesky decomposition of $E[\mathbf{E}(t)\mathbf{E}^T(t)]$. Multiplying both sides of Eq. 15 by $\mathbf{S}^{-1}(t)$, one gets:

$$\mathbf{Y}(t) = \mathbf{X}(t)\boldsymbol{\beta}(t) + \boldsymbol{\xi}(t), \tag{16}$$

where

$$\mathbf{Y}(t) = \mathbf{S}^{-1}(t) \begin{bmatrix} \mathbf{F}(t)\hat{\mathbf{x}}(t-1) \\ y(t) \end{bmatrix},$$

$$\mathbf{X}(t) = \mathbf{S}^{-1}(t) \begin{bmatrix} \mathbf{I}_M \\ \mathbf{H}(t) \end{bmatrix},$$

$\boldsymbol{\beta}(t) = \mathbf{x}(t)$ and $\boldsymbol{\xi}(t) = -\mathbf{S}^{-1}(t)\mathbf{E}(t)$. Here, the multiplication of $\mathbf{E}(t)$ by $\mathbf{S}^{-1}(t)$ can be treated as the whitening of $\mathbf{E}(t)$, and hence the residual $\boldsymbol{\xi}(t)$ satisfies $E[\boldsymbol{\xi}(t)\boldsymbol{\xi}^T(t)] = \mathbf{I}_{M+1}$. Eq. 16 is a standard linear regression problem with LS solution:

$$\hat{\boldsymbol{\beta}}(t) = \hat{\mathbf{x}}(t/t) = [\mathbf{X}^T(t)\mathbf{X}(t)]^{-1}\mathbf{X}^T(t)\mathbf{Y}(t), \tag{17}$$

and the covariance matrix of estimating $\hat{\boldsymbol{\beta}}(t)$ is

$$E\left[\left(\boldsymbol{\beta}(t) - \hat{\boldsymbol{\beta}}(t)\right)\left(\boldsymbol{\beta}(t) - \hat{\boldsymbol{\beta}}(t)\right)^T\right] = \mathbf{P}(t/t) = [\mathbf{X}^T(t)\mathbf{X}(t)]^{-1}. \tag{18}$$

It was shown in [5, 10] that Eqs. 16–18 form an equivalent Kalman filtering algorithm based on LS criterion with $\hat{\boldsymbol{\beta}}(t) = \hat{\boldsymbol{x}}(t/t)$ and $\boldsymbol{P}(t/t) = \text{cov}(\hat{\boldsymbol{\beta}}(t))$. As seen in Eq. 16, the lower part of the equation is a conventional LS estimation of $\boldsymbol{x}(t)$ from the current measurement $y(t)$ and the upper part is a regularization term that imposes a smoothness constraint from the state dynamic into the LS problem. Consequently, if fewer measurements are used to update the state vector, the bias error is low especially when the system state is fast varying. On the other hand, if the state is time-invariant or slow varying, more measurements are used to track the state vector and reduce the estimation variance. As mentioned in Sect. 1, the conventional Kalman filter-based PSD methods in [1, 8, 9] only use one measurement to update the state estimate. Therefore, these methods often have a relatively large state estimation variance and degraded frequency resolution in the case of slowly time-varying frequency components where more measurements should have been used to reduce the estimation variance.

The KFVNM is obtained as follows. Consider a block of measurements lying in a symmetric window centered at $y(t)$, $[y(t-L), \dots, y(t), \dots, y(t+L)]$, where $h = 2L+1$ is the total number of measurements, or window size. Including all these measurements in Eq. 16 for state estimation, we get:

$$\bar{\boldsymbol{Y}}(t) = \bar{\boldsymbol{X}}(t)\boldsymbol{\beta}(t) + \bar{\boldsymbol{\xi}}(t), \quad (19)$$

where

$$\bar{\boldsymbol{Y}}(t) = \bar{\boldsymbol{S}}^{-1}(t) \begin{bmatrix} \boldsymbol{F}(t)\hat{\boldsymbol{x}}(t-1) \\ \boldsymbol{y}(t) \end{bmatrix}, \quad \bar{\boldsymbol{X}}(t) = \bar{\boldsymbol{S}}^{-1}(t) \begin{bmatrix} \boldsymbol{I}_M \\ \bar{\boldsymbol{H}}(t) \end{bmatrix},$$

$$\boldsymbol{y}(t) = [y(t-L), \dots, y(t), \dots, y(t+L)]^T, \text{ and}$$

$$\bar{\boldsymbol{H}}(t) = [\boldsymbol{H}^T(t-L), \dots, \boldsymbol{H}^T(t), \dots, \boldsymbol{H}^T(t+L)]^T.$$

Here, $\bar{\boldsymbol{S}}(t)$ is obtained from the Cholesky decomposition of

$$\begin{bmatrix} \boldsymbol{P}(t/t-1) & & 0 \\ & \text{diag}\{\boldsymbol{R}(t-L), \dots, \boldsymbol{R}(t), \dots, \boldsymbol{R}(t+L)\} & \end{bmatrix}$$

in the new algorithm, and it acts as a weighted matrix to let the residual $\bar{\boldsymbol{\xi}}(t)$ satisfy $E[\bar{\boldsymbol{\xi}}(t)\bar{\boldsymbol{\xi}}^T(t)] = \boldsymbol{I}_{M+h}$. Similarly, the LS solution of Eq. 19 can be obtained by:

$$\hat{\boldsymbol{\beta}}(t) = \hat{\boldsymbol{x}}(t/t) = [\bar{\boldsymbol{X}}^T(t)\bar{\boldsymbol{X}}(t)]^{-1}\bar{\boldsymbol{X}}^T(t)\bar{\boldsymbol{Y}}(t), \quad (20)$$

$$\boldsymbol{P}(t/t) = [\bar{\boldsymbol{X}}^T(t)\bar{\boldsymbol{X}}(t)]^{-1}. \quad (21)$$

Therefore, PSDs with different time-frequency properties can be obtained. Using these results, the number of measurements h can be varied to handle different time and frequency variations in the target time series.

To handle the window selection problem, the intersection of confidence intervals (ICI) rule [16] is employed to

generate an adaptive PSD. Generally, an optimal local window size should minimize the mean squared error (MSE), which is the sum of estimated bias and variance. The MSE can be expressed as a function of the window size. The ICI method finds the optimal window size by examining the confidence intervals of the estimates when the window size in a finite window size set gradually increases. For a small window size h , we expect that the bias of estimation will be small and the confidence interval will gradually decrease with increasing value of h while the center of the interval remains more or less fixed. When h is increased to a certain point, a large bias will result and the center of the interval will shift significantly, while the length of interval will be small. As a result, the confidence interval will no longer intersect those with smaller values of h . The ICI bandwidth selection method computes and examines the confident intervals in order to detect this sudden change and hence the optimal window size. More details about the ICI rule can be found in [16] and references therein.

Suppose that we are given a finite set of window sizes in ascending order of magnitude:

$$\boldsymbol{h} = \{h_k, k = 1, 2, \dots, K \mid h_1 < h_2 < \dots < h_K\}. \quad (22)$$

For each window size h_k , we will obtain a Kalman filter-based spectral density $\mathcal{P}(t, f; h_k)$. The variance, $\text{Var}(\cdot)$, and the bias, $\text{bias}(\cdot)$, of $\mathcal{P}(t, f; h_k)$ are functions of the time window h_k . Therefore, the corresponding mean square error ($\text{MSE}(\cdot)$) is given by:

$$\text{MSE}(t, f; h_k) = \text{Var}[\mathcal{P}(t, f; h_k)] + \text{bias}^2[\mathcal{P}(t, f; h_k)]. \quad (23)$$

Since the estimation variance is a decreasing function and the bias is an increasing functions of the window size h_k , there exists an optimal window h_{opt} such that two terms are equal and hence $\text{MSE}(t, f; h_k)$ is minimized. To determine h_{opt} , the ICI rule examines a sequence of confidence intervals of the estimates $\mathcal{P}(t, f; h_k)$:

$$D_k = [L_k, U_k], \quad (24)$$

where $L_k = \mathcal{P}(t, f; h_k) - \Gamma \cdot \sigma(h_k)$, $U_k = \mathcal{P}(t, f; h_k) + \Gamma \cdot \sigma(h_k)$, $\sigma^2(h_k) = \text{Var}[\mathcal{P}(t, f; h_k)]$ is the variance of the estimate using the window length h_k , and $\Gamma > 0$ is a threshold parameter of the confidence interval. According to [6], the variance of $\mathcal{P}(t, f; h_k)$ with a window size (number of measurements) h_k can be computed approximately as:

$$\begin{aligned} \sigma^2(h_k) &= \text{Var}(\mathcal{P}(t, f; h_k)) \\ &= \frac{[Y_{\mathcal{P}}(t, f; h_k)]^{3/2}}{2} \sqrt{\frac{\boldsymbol{p}e^{\boldsymbol{H}}(f)\hat{\sigma}_\delta^2(t; h_k)\boldsymbol{e}(f)}{\hat{\sigma}_e^2(t; h_k)}}, \end{aligned} \quad (25)$$

where $\hat{\sigma}_\delta^2(t; h_k)$ and $\hat{\sigma}_e^2(t; h_k)$ are respectively the estimated variances of state noise and observation noise.

Define the following quantities from the confidence intervals:

$$\bar{L}_k = \max \{ \bar{L}_{k-1}, L_k \}; \bar{L}_0 = 0 \text{ and,} \tag{26}$$

$$\underline{U}_k = \min \{ \underline{U}_{k-1}, U_k \}; \underline{U}_0 = 0, \tag{27}$$

for $k = 1, 2, \dots, K$. The objective is to find h_k such that $\underline{U}_k \geq \bar{L}_k$ for the largest possible value of k . By using an adaptive window for each time-frequency sample, a better tradeoff between time and frequency resolutions can be achieved for various signal components possibly with different time-frequency variations. Therefore, the adaptive PSD is expected to provide clearer time-frequency contents than that with a fixed window size.

3 Results

3.1 Analysis of synthetic pressure signal

Synthetic biomedical signal models are important tools in biomedical signal analysis. The ability to simulate signals with realistic characteristics enables us to develop and test our algorithms and methodologies on synthetic signals prior to validation on real data. Since the statistical properties and other characteristics of the synthetic data are known, it provides the gold standard to quantitatively evaluate the performance of different algorithms as shown below.

Consider the following three criteria C1, C2 and C3, which can be respectively regarded as a measure of the bias, variance and MSE of the PSD estimate between true and extracted representations:

$$C1 : C_1(t) = N^{-1} \left[\sum_{n=1}^N f_{\text{ext}}(t, n) \right] - f(t), \tag{28}$$

$$C2 : C_2(t) = N^{-1} \sum_{n=1}^N \left[f_{\text{ext}}(t, n) - N^{-1} \sum_{n=1}^N f_{\text{ext}}(t, n) \right]^2, \tag{29}$$

$$C3 : C_3(t) = N^{-1} \sum_{n=1}^N [f_{\text{ext}}(t, n) - f(t)]^2, \tag{30}$$

where N is the number of independent realizations, $f_{\text{ext}}(t, n)$ corresponds to the extracted (or estimated) frequency at the t -th time instant during the n -th realization, $f(t)$ is the true frequency at the t -th time instant. Here, $f_{\text{ext}}(t, n)$ is determined by the peak position of the estimate. The smaller these values, the better the estimation algorithm is. For known test signals, the time-frequency resolution can be measured by comparing the MSE of the estimator $f_{\text{ext}}(t, n)$ (extracted from the estimated PSDs) with the ground true

$f(t)$ which is given by C3. Whereas C1 and C2 measure respectively the bias and variance of $f_{\text{ext}}(t, n)$.

As an illustration, we shall consider the statistical model developed in [1] for simulating the pressure signals such as ABP and ICP signals. In this model, the signal generated is composed of two fundamental sinusoids, namely cardiac and respiratory frequencies. The effects of respiration such as pulse amplitude variation and respiratory sinus arrhythmia are considered as amplitude and frequency modulations of the fundamental cardiac sinusoidal signal, respectively. More precisely, the signal model is given by:

$$s(t) = A_c [1 + pr(t)] \cdot [\alpha \cos(2\pi f_c t + q \sin 2\pi f_r t) + \beta \cos(4\pi f_c t + qb \sin 2\pi f_r t + \theta)] + \kappa_r \cdot r(t), \tag{31}$$

where A_c is the cardiac amplitude, p is the amplitude modulation index, $r(t) = \cos(2\pi f_r t)$ is the respiratory signal, f_c and f_r are respectively the fundamental cardiac and respiratory frequencies, q is the frequency modulation index, α and β are respectively the first and second cardiac component amplitudes, θ is the phase difference between the first and second harmonics of cardiac frequency and κ_r is the additive respiration amplitude. For simplicity, only the first two harmonics in cardiac frequency are considered in Eq. 31 because most of the power in real pressure signals is contained in these two harmonics. The values of various parameters used in this example are: $A_c = 1$, $p = 0.01$, $q = 0.01$, $\alpha = 0.1$, $\beta = 0.09$, $\theta = 0.3\pi$, and $\kappa_r = 0.4$.

The testing procedure involves the generation of $N = 100$ realizations of the same random process using the statistical model in Eq. 31. The sampling rate and the time duration for this experimental signal are set to 12.5 Hz and 20 s, respectively. To illustrate the effectiveness of the proposed algorithm, the synthetic signals are designed to contain a sudden change of cardiac and respiratory frequencies at the time instant around 10 seconds as shown in Fig. 1a. The window sizes h in Eq. 22 are chosen as $h = \{1, 9, 17, 33\}$. The synthetic signal is corrupted by a zero mean additive white Gaussian noise with a SNR of 30 dB. The model order M is important to the accuracy of AR coefficient estimates and the frequency resolution of the PSD estimation. A small model order cannot discriminate different frequency components. On the other hand, when the model order is too large spurious peaks may appear around the true frequency. According to [7], for a noise-free signal consisted of m sinusoidal components, a real AR(2m) model is required. In addition, the model order should increase with the amount of additive noise. In this experiment, the AR order is chosen as $M = 7$ for the synthetic signal composed of three sinusoidal components and small noise component.

As a comparison, four time-frequency analysis algorithms were considered: 1) the Kalman filter-based PSD

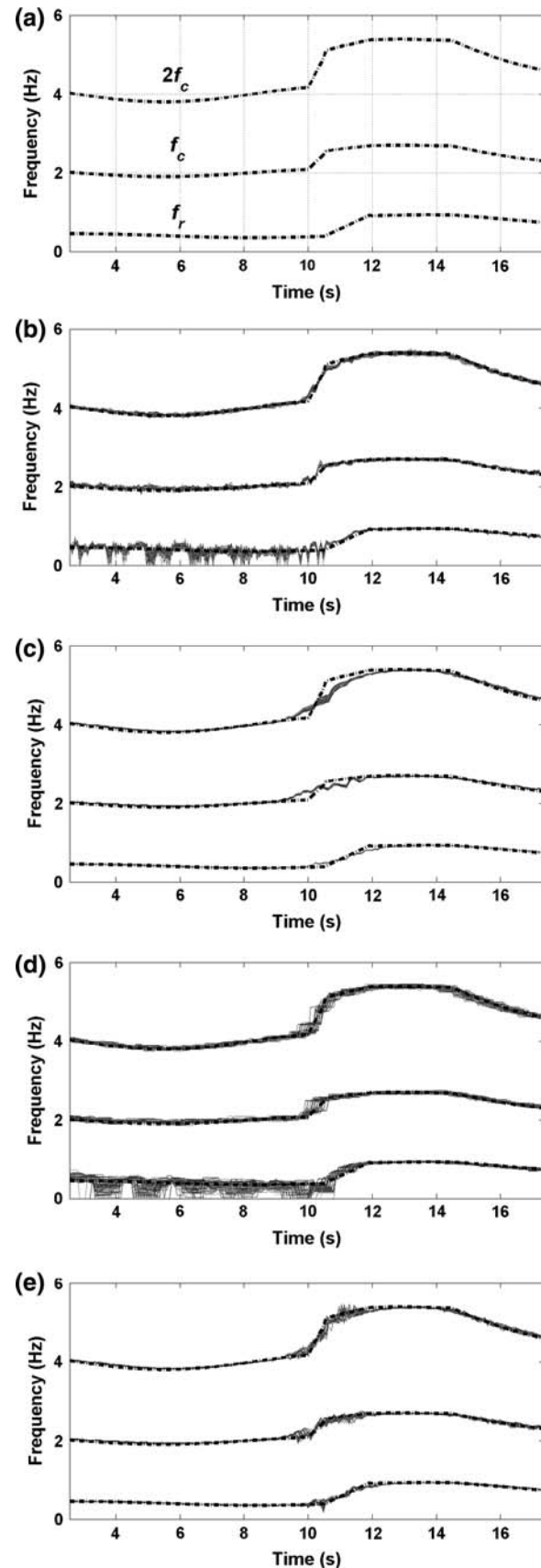
Fig. 1 Performance comparison between different PSD estimation methods for the synthetic signal: (a) true frequency contents of the synthetic signal (f_c : cardiac frequency, f_r : respiratory frequency), and extracted frequency contents using (b) Kalman filter with one measurement (A1), (c) Kalman filter with 33 measurements (A2), (d) dual Kalman filter studied in [1] (A3), and (e) the proposed algorithm (A4)

estimation algorithm with one measurement (A1), 2) the Kalman filter-based PSD estimation algorithm with 33 measurements (A2), 3) the dual Kalman filter-based PSD estimation algorithm plus averaging operation over ten time samples studied in [1] (A3), 4) and the proposed algorithm (A4). In Figs. 1b – 1e, the results of 100 independent realizations using the four algorithms are overlaid and each curve represents the peak position of the PSD estimate in three frequency bands, 0–1.3, 1.3–3.3 and 3.3–6 Hz, where the three components are supposed to lie. It can be seen in Fig. 1b that a large window size can provide more precise time information at the expense of poor frequency representation, and vice versa in Fig. 1c. Also, the proposed algorithm offers much less deviation from the true values as compared with other algorithms.

Our assessment study also included a quantitative comparison of the four methods using the C1, C2 and C3 criteria. For clarity, the frequency band is also divided into three intervals, 0–1.3, 1.3–3.3 and 3.3–6 Hz, and the obtained values are plotted in logarithmic scale. Note that since the criterion C1 may be negative, we used the absolute value for the purposes of comparison. The results in terms of the above criteria are shown in Fig. 2 and the average value of $C_k(i)$ over the total number of time samples (denoted by \bar{C}_k), $k = 1, 2, 3$, are summarized in Table 1. As expected, it can be seen from Fig. 2a that the criteria C1, C2 and C3 for the algorithm A1 are relatively large for slowly time-varying frequency components especially in the frequency interval 0–1.3 Hz, which is opposite to the observations for the algorithm A2. Moreover, Fig. 2c shows that algorithm A3 provides insignificant improvement in criterion C3 over the algorithm A1 for slowly time-varying frequency components, and its performance during the sudden change of frequency (i.e. at around time instant 10) is considerably degraded due to the averaging operation. On the other hand, the proposed algorithm appears to have good performance in most cases. This suggests that the proposed algorithm is capable of achieving a better performance than conventional PSD estimation methods.

3.2 Analysis of a nonstationary ICP signal

In this section we present a representative example of the results obtained when the proposed method was used to



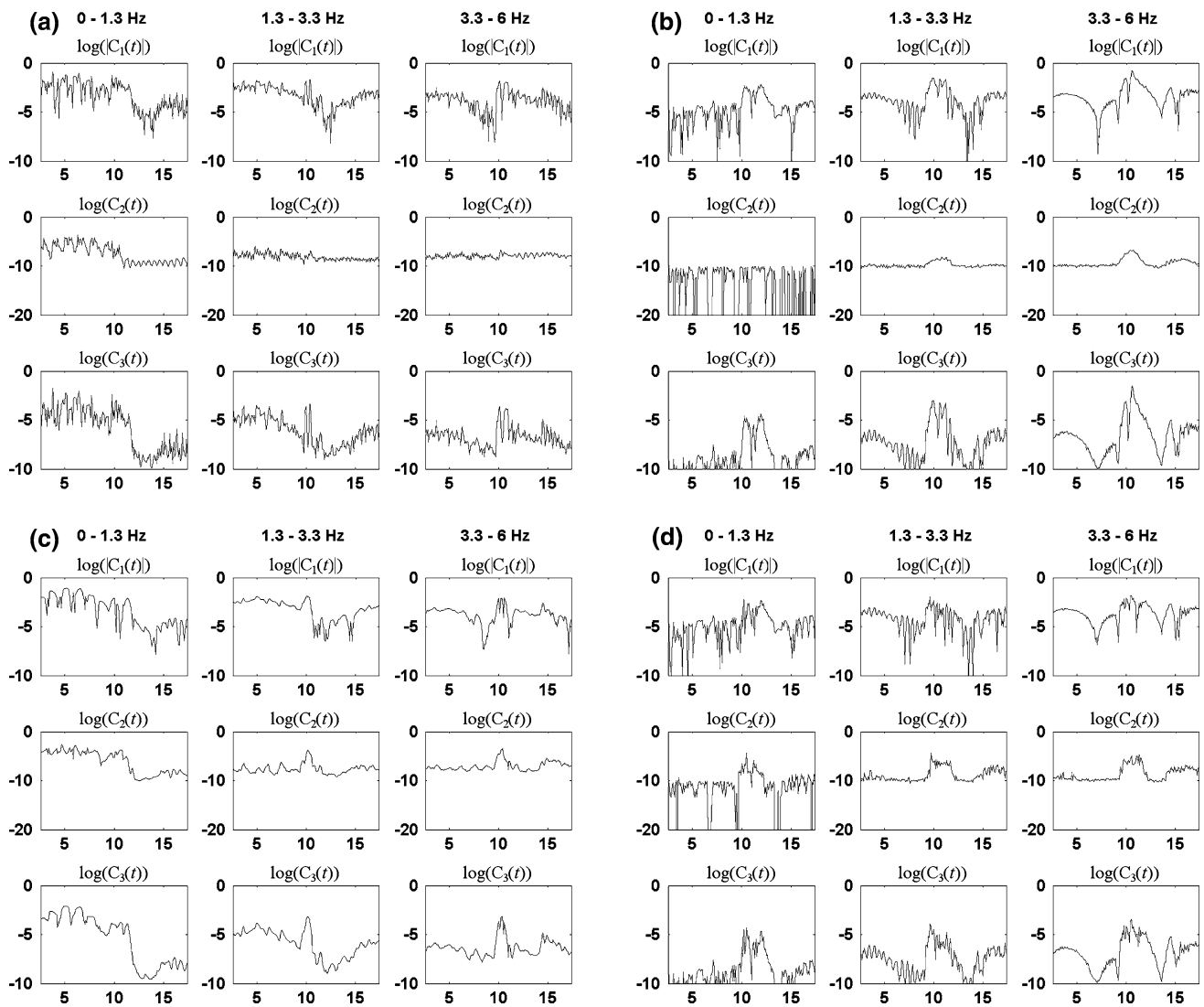


Fig. 2 Performance comparison between (a) Kalman filter-based PSD estimation algorithm with one measurement (A1), (b) Kalman filter-based PSD estimation algorithm with 33 measurements (A2), (c) dual Kalman filter-based PSD estimation algorithm plus averaging

operation over ten time samples studied in [1] (A3), and (d) the proposed algorithm (A4). The *x*-axis denotes the time in second, and the *y*-axis is in a logarithmic scale

Table 1 Bias (\bar{C}_1), variance (\bar{C}_2) and mean square error (\bar{C}_3) of various algorithms

	0–1.3 Hz				1.3–3.3 Hz				3.3–6 Hz			
	A1	A2	A3	A4	A1	A2	A3	A4	A1	A2	A3	A4
\bar{C}_1	4.53	1.19	−33.3	0.24	37.9	22.6	−35.8	21.5	−6.11	−6.91	−6.03	0.32
\bar{C}_2	4.93	0.03	13.2	0.34	0.82	0.13	2.41	0.86	1.31	0.23	4.02	1.13
\bar{C}_3	13.1	1.54	20.3	1.38	4.59	4.25	4.19	2.51	5.41	7.84	5.42	5.17

All the values are normalized by 10^{-3}

analyze cardiovascular pressure signals. For illustration purposes we analyzed the same ICP signal used in other PSD estimation works involving the use of the Kalman filtering framework [1].

Fig. 3a shows the target signal recorded from a selected patient who suffered from a period of intracranial

hypertension and was treated by a therapy involving mechanical hyperventilation to reduce elevated ICP. As seen from Fig. 3a, the sudden change in mean ICP is due to the hyperventilation intervention occurred approximately after 800 s. Previous works have shown that nonparametric methods such as Welch’s may not be able to provide

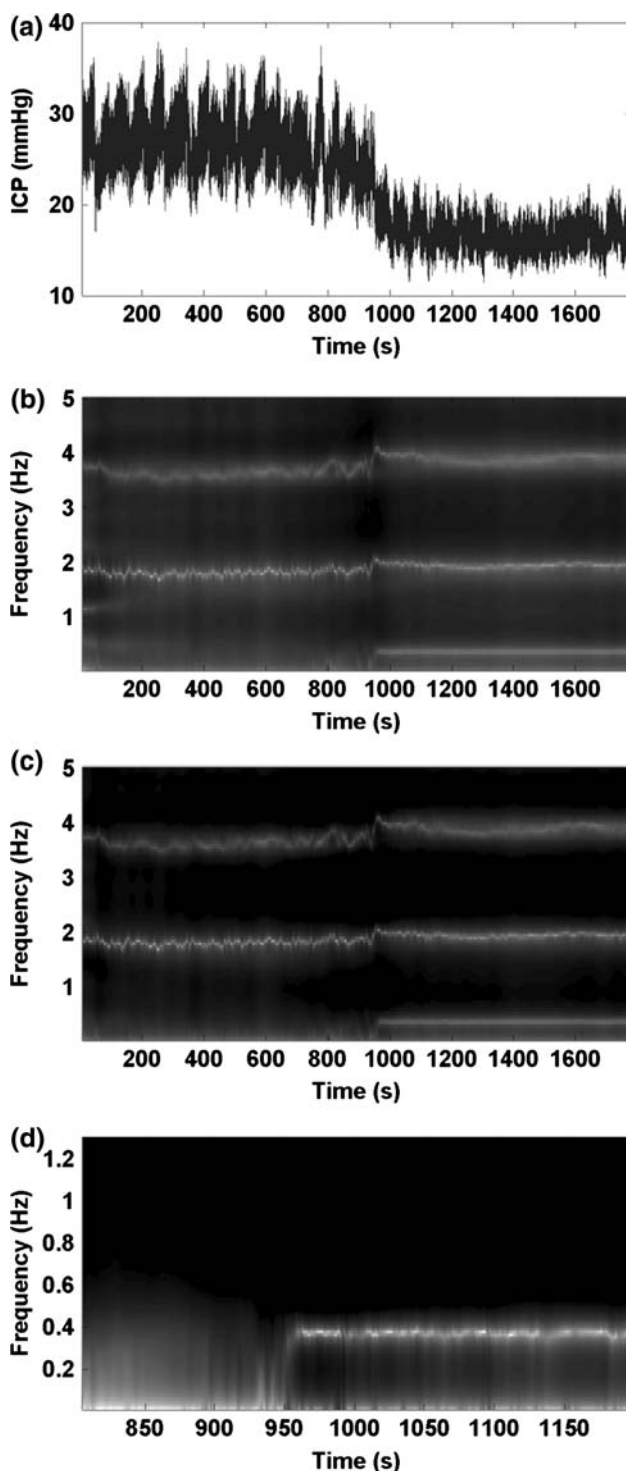


Fig. 3 **a** Real ICP signal, **b** PSD estimated using the Kalman filter-based algorithm with one measurement (A1), **c** PSD estimated using the proposed Kalman filter-based algorithm, **d** PSD of the respiratory component around 950 s

sufficient time and frequency resolutions for the determination of the time instant when the hyperventilation intervention occurred [1]. Prior to the application the PSD estimation algorithm, the signal was decimated to 12.5 Hz

by passing through a lowpass filter and a downsampler. As suggested in [17], this operation not only reduces the computational complexity, but also enhances the SNR because the noise outside the frequency of interest is attenuated. As compared with the synthetic signal in the previous example, the real signal has relatively larger amplitude variation and slower rate of change of the frequency components. This results in a higher AR order and longer data windows required to track the signal changes. The AR order is selected as $M = 25$ in a trial and error manner because of unknown SNR. The window size is chosen as $h = \{1, 17, 33, 65\}$. Figs. 3b and 3c show the PSD estimation results obtained respectively by the algorithm A1 and the proposed algorithm. It can be seen that PSD estimated by the proposed approach exhibits less spectral variations especially in slowly time-varying components. Both figures also show that the cardiac component and its harmonic are present around 2 and 4 Hz, whereas the respiratory component is found in the frequency band ranging from 0 to 0.5 Hz. A sudden change of frequency in the three components can be observed at about 950 s. To examine the change of the respiratory rate after hyperventilation, in Fig. 3c we show the time-frequency distribution of the ICP signal focusing on the time of the hyperventilation (800 – 1200 s) and the frequency of the respiratory component (0–1.3 Hz). Comparing with the results in [1], the proposed algorithm offers a clearer time-frequency contents and fewer spurious components in the estimated PSD, due to the use of variable number of measurements.

4 Discussion and conclusions

A new Kalman filter with variable number of measurements (KFVNM) algorithm is described in this paper to estimate the PSD of nonstationary pressure signals. By employing the ICI rule to choose the appropriate window size adaptively, the proposed KFVNM-based PSD estimation method is expected to provide better time-frequency resolution than conventional Kalman filter-based methods.

To illustrate the effectiveness of the proposed KFVNM-based PSD estimation method, it was first validated in Sect. 3.1 quantitatively using synthetic cardiovascular pressure signals. We compared various conventional Kalman filter-based PSD estimation methods and assessed their performances using the defined quantitative measures in Eqs. 28–30. Since the characteristics of synthetic signal are known, the time-frequency resolution can be measured by comparing the MSE (C3) of the estimator (extracted from the estimated PSDs) with the ground true. Whereas C1 and C2 measure respectively the bias and variance of

the estimator. It can be seen that the proposed method is capable of providing more accurate time-frequency contents than conventional methods and the improved accuracy was shown quantitatively by the criteria C1, C2 and C3.

Apart from synthetic signal, the algorithm was applied to a representative ICP signal, which contains both temporal and spectral information due to the hyperventilation intervention. The results in Sect. 3.2 suggest that the proposed method is able to achieve better tradeoff between time and frequency resolutions and enhance higher accuracy of the extracted features than the conventional Kalman filter-based PSD estimation methods. The good time-frequency resolution of the proposed method would allow us to give reasonable estimation of frequency component and detection of important events. Therefore, time-frequency analysis of such kind of signal using the proposed method would provide a more complete understanding on the changes in time and frequency characteristics. For example, as shown in Fig. 3, we can observe how the heart rate increased slightly and became more constant. We can also note how the heart rate went from about 1.8 to 2 Hz (i.e. 120 beats/min) and the heart rate variability decreased once hyperventilation was initiated.

Besides, it is also possible to apply the proposed method to analyze time-frequency characteristics of other signals having a similar nature (single- or multi-component sinusoids with reasonable amount of additive noise), because AR processes can accurately model narrowband stochastic signals. These include various biomedical signals and there is a primary interest in estimating the temporal and spectral information. To apply the proposed method for the analysis of other kinds of signals, the AR model order should be carefully determined according to the number of sinusoids contained in the signals and the amount of noise.

Compared with the conventional Kalman filter-based PSD estimation, the proposed method has higher computational complexity because it needs the calculation of a series of Kalman filter-based PSD estimation with different number of measurements and selection of the appropriate number of measurements. However, for offline signal processing, it is desired to obtain a clearer time-frequency representation for the better understanding of the testing signal at the expense of a relatively higher computational complexity.

Acknowledgments The authors would thank Dr. Chang Chunqi for his suggestions on this manuscript. This work has been supported by the general research fund of the Hong Kong research grant council.

References

1. Aboy M, Marquez OW, McNamers J, Hornero R, Thong T, Goldstein B (2005) Adaptive modeling and spectral estimation of nonstationary biomedical signals based on Kalman filtering. *IEEE Trans Biomed Eng* 52(8):1485–1489
2. Aboy M, McNamers J, Hornero R, Thong T, Cuesta D, Novak D, Goldstein B (2004) A novel statistical model for simulation of arterial and intracranial pressure. *Conf Proc IEEE Eng Med Biol Soc* 2004:129–132
3. Akay M (1998) Time frequency and wavelets in biomedical signal processing. IEEE Press, New York
4. Cohen L (1995) Time frequency analysis. Prentice, Upper Saddle River, pp 113–177
5. Durović ŽM, Kovačević BD (1999) Robust estimation with unknown noise statistics. *IEEE Trans Automat Contr* 44(6):1292–1296
6. Gustafsson BD, Gunnarsson S, Ljung L (1995) A parametric method for modeling of time varying spectral properties. Technical report LiTH-ISY-R-1709, Department of Electrical Engineering, Linköping University
7. Kay SM (1998) Modern spectral estimation: theory and application. Prentice-Hall, Englewood Cliffs
8. Kitagawa G (1983) Changing spectrum estimation. *J Sound Vib* 89(4):433–445
9. Kitagawa G, Gersch W (1985) A smoothness priors time-varying AR coefficient modeling of nonstationary covariance time series. *IEEE Trans Automat Contr* 30(1):48–56
10. Kovačević BD, Durović ŽM, Glavašhi ST (1992) On robust Kalman filtering. *Int J Contr* 3:547–562
11. Mallat S (1998) A wavelet tour of signal processing. Academic Press, San Diego, pp 76–87
12. Manolakis DG, Ingle VK, Kogan SM (2000) Statistical and adaptive signal processing. McGraw-Hill, New York, pp 195–260, 445–498
13. Proakis J, Rader C, Ling F, Nikias C, Moonen M, Proudler I (2002) Algorithms for statistical signal processing. Prentice-Hall, Englewood Cliffs, pp 432–503
14. Qian S (2002) Introduction to time frequency and wavelet transforms. Prentice-Hall, Englewood Cliffs, pp 99–146
15. Rangayyan RM (2002) Biomedical signal analysis: a case-study approach. Wiley, New York, pp 277–444
16. Stanković L, Katkovnik V (1999) The Wigner distribution of noisy signals with adaptive time-frequency varying window. *IEEE Trans Signal Process* 47(4):1099–1108
17. Tkacenko A, Vaidyanathan PP (2001) The role of filter bank in sinusoidal frequency estimation. *J Franklin Inst* 338:517–547